Oncogene (2019) 38:4512–4526
https://doi.org/10.1038/s41388-019-0734-5

ARTICLE

Targeting SYK signaling in myeloid cells protects against liver fibrosis and hepatocarcinogenesis

Alejandro Torres-Hernandez[1] · Wei Wang[1] · Yuri Nikiforov[1] · Karla Tejada[1] · Luisana Torres[1] · Aleksandr Kalabin[1] · Yue Wu[1] · Muhammad Israr Ul Haq[1] · Mohammed Y. Khan[1] · Zhen Zhao[1] · Wenyu Su[1] · Jimmy Camargo[1] · Mautin Hundeyin[1] · Brian Diskin[1] · Salma Adam[1] · Juan A. Kochen Rossi[1] · Emma Kurz[1] · Berk Aykut[1] · Sorin A. A. Shadaloey[1] · Joshua Leinwand[1] · George Miller[1,2]

Received: 14 November 2018 / Revised: 2 January 2019 / Accepted: 4 January 2019 / Published online: 11 February 2019

Abstract

Liver fibrosis and fibrosis-associated hepatocarcinogenesis are driven by chronic inflammation and are leading causes of morbidity and death worldwide. SYK signaling regulates critical processes in innate and adaptive immunity, as well as parenchymal cells. We discovered high SYK expression in the parenchymal hepatocyte, hepatic stellate cell (HSC), and the inflammatory compartments in the fibrotic liver. We postulated that targeting SYK would mitigate hepatic fibrosis and oncogenic progression. We found that inhibition of SYK with the selective small molecule inhibitors Piceatannol and PRT062607 markedly protected against toxin-induced hepatic fibrosis, associated hepatocellular injury and intra-hepatic inflammation, and hepatocarcinogenesis. SYK inhibition resulted in increased intra-tumoral expression of the p16 and p53 but decreased expression of Bcl-xL and SMAD4. Further, hepatic expression of genes regulating angiogenesis, apoptosis, cell cycle regulation, and cellular senescence were affected by targeting SYK. We found that SYK inhibition mitigated both HSC trans-differentiation and acquisition of an inflammatory phenotype in T cells, B cells, and myeloid cells. However, in vivo experiments employing selective targeted deletion of SYK indicated that only SYK deletion in the myeloid compartment was sufficient to confer protection against fibrogenic progression. Targeting SYK promoted myeloid cell differentiation into hepato-protective $TNF\alpha^{low}$ $CD206^{hi}$ phenotype downregulating mTOR, IL-8 signaling and oxidative phosphorylation. Collectively, these data suggest that SYK is an attractive target for experimental therapeutics in treating hepatic fibrosis and oncogenesis.

Introduction

Liver fibrosis, which can progress to cirrhosis and liver cancer, is a leading cause of death worldwide [1]. Hepatic fibrosis represents the pathologic sequela of chronic repetitive injury. Viral infection, obesity-related steatohepatitis, and alcoholism are major risk factors for the development of liver fibrosis and oncogenic progression [2]. Hepatic stellate cell (HSC) activation is a key event necessary for liver fibrogenesis [3]. Innate immune signaling also plays an important role in regulating this process. Natural killer cells suppress liver fibrosis by directly killing activated HSCs [4]. By contrast, TNF-α expressing macrophages promote hepatic inflammation leading to HSC activation. TGF-β1 is also secreted by macrophages and initiate a robust fibrogenic cascade by further activating HSCs [5]. Liver resident macrophages and recruited macrophages additionally promote HSC survival in an NF-κB–dependent manner [6].

These authors contributed equally: Alejandro Torres-Hernandez, Wei Wang

Supplementary information The online version of this article (https://doi.org/10.1038/s41388-019-0734-5) contains supplementary material, which is available to authorized users.

✉ George Miller
george.miller@nyumc.org

[1] S.A. Localio Laboratory, Departments of Surgery, New York University School of Medicine, 450 East 29th Street, New York, NY 10016, USA

[2] Departments of Cell Biology, New York University School of Medicine, 450 East 29th Street, New York, NY 10016, USA

However, the cell signaling mechanisms governing myeloid cell differentiation and macrophage phenotype in liver fibrosis and hepatocarcinogenesis remain incompletely understood.

Spleen tyrosine kinase (SYK) is a 72 kDa signaling molecule that is widely expressed in both hematopoietic and non-hematopoietic cells and plays an important role in relaying adaptive immune signals and mediating innate immune recognition [7]. Initially discovered in B-cells, SYK signaling has been described in T cells, myeloid cells, and epithelial cells [7, 8]. SYK is a signaling intermediary for a variety of receptors, including the B-cell receptor and the C-type lectin receptors Mincle and Dectin-1. We previously reported that Dectin-1 signaling is protective against liver fibrosis and progression to liver cancer by suppressing TLR4 signaling pathways via promotion of macrophage colony stimulating factor (M-CSF) expression [9]. As such, deletion of Dectin-1 exacerbated hepatic fibrosis and hepatocarcinogenesis. By contrast, a recent report showed that directly targeting SYK protected against chronic liver injury in hepatitis B virus (HBV)-infected, hepatitis C virus (HCV)-infected and non-alcoholic steatohepatitis liver tissues [10]. Our goal was to evaluate the mechanistic role of SYK signaling on the fibrosis—hepatocarcinogenesis axis and specifically determine its modulatory role in this process in each cellular population including liver parenchymal cells, HSCs, myeloid cells, B lymphocytes, and T lymphocytes.

Results

High SYK signaling in liver fibrosis

We discovered robust SYK expression in primary hepatocytes, hepatic leukocytes, and hepatic stellate cells (HSC) on confocal microscopy (Fig. 1a–c). Western blotting suggested increased p-SYK expression in vivo in fibrotic liver tissues (Fig. 1d). CCl_4 treatment similarly increased p-SYK expression in vitro in cultured hepatocytes (Fig. 1e). However, select leukocyte subsets, including B cells, $CD4^+$ T cells, and NKT cells, downregulated p-SYK expression in hepatic fibrosis (Fig. 1f) suggesting that increased global SYK expression is likely the result of higher inflammatory cell recruitment (Fig. 1g).

Inhibition of SYK is protective against liver fibrosis

To determine the influence of SYK signaling on liver fibrosis, we serially treated mice with the SYK inhibitor Piceatannol or vehicle during the 12-week course of TAA-induced fibrosis. Piceatannol mitigated liver fibrosis based on gross appearance of livers, histological analysis using H&E, Trichrome, Sirius Red staining, α-SMA immunohistochemistry, serum transaminase levels, and liver hydroxyproline content (Fig. 2a–g). The inflammatory infiltrate was also reduced (Fig. 2h). Protein (Fig. 2i) and RNA-based (Fig. 2j) analyses confirmed that SYK inhibition results in diminished hepatic expression of extracellular matrix proteins and inflammatory and tissue modulators of fibrosis. SYK inhibition did not affect the tissue histology, transaminase levels, hydroxyproline content, or inflammatory infiltrate in non-fibrotic liver (Figure S1). Further, SYK inhibition was also protective against the intrahepatic inflammation associated with liver fibrosis as evidenced by diminished pan-leukocyte, macrophage, B cell, and neutrophil infiltration (Fig. 2h and Fig. S2). Treatment using PRT062607 (PRT), a more selective SYK inhibitor, was similarly protective against hepatic fibrosis, hepatocellular injury, and inflammation (Fig. 3).

Inhibition of SYK is protective against hepatocellular carcinoma

Since liver fibrosis is the primary risk factor for hepatocarcinogenesis, we postulated that SYK inhibition would also mitigate malignant transformation in the fibrotic liver. To test this, we employed the CCL_4 + Diethylnitrosamine (DEN) model [11]. Consistent with our hypothesis, SYK inhibition protected mice from liver cancer development and concomitant fibrosis and hepatocellular damage (Fig. 4a–e). SYK inhibition again mitigated intrahepatic inflammation in mice treated with CCL_4 + DEN (Fig. 4f). Analysis of hepatic expression of tumor suppressor or cell cycle regulatory genes demonstrated that Piceatannol-treated liver exhibited increased expression of the p16 and p53 tumor suppressor genes and decreased expression of Bcl-xL and SMAD4 (Fig. 4g). Further, hepatic expression of genes involved in angiogenesis (*Angpt2*, *Ccl2*), apoptosis (*Apaf1*, *Bcl2l11*, *Birc3*, *Casp7*), cell cycle regulation (*Mki67*, *Ccnd2*), and cellular senescence (*Map2k1*, *Serpinb2*) were altered by Piceatannol treatment (Fig. 4h). *SYK* expression did not correlate with outcome in human liver cancer based on analysis of the Human Protein Atlas database (Fig. 4i).

Inhibition of SYK mitigates HSC activation

We postulated that SYK inhibition may be protective by mitigating activation of the fibrogenic and inflammatory compartments. To test whether SYK signaling promotes HSC transdifferentiation, we employed in vitro modeling. SYK inhibition impeded HSC migration in a scratch assay (Fig. 5a). Similarly, Piceatannol mitigated HSC cellular proliferation (Fig. 5b). SYK inhibition also prevented HSC mobilization in a transwell assay (Fig. 5c). We and others have previously shown that HSC transdifferentiate in

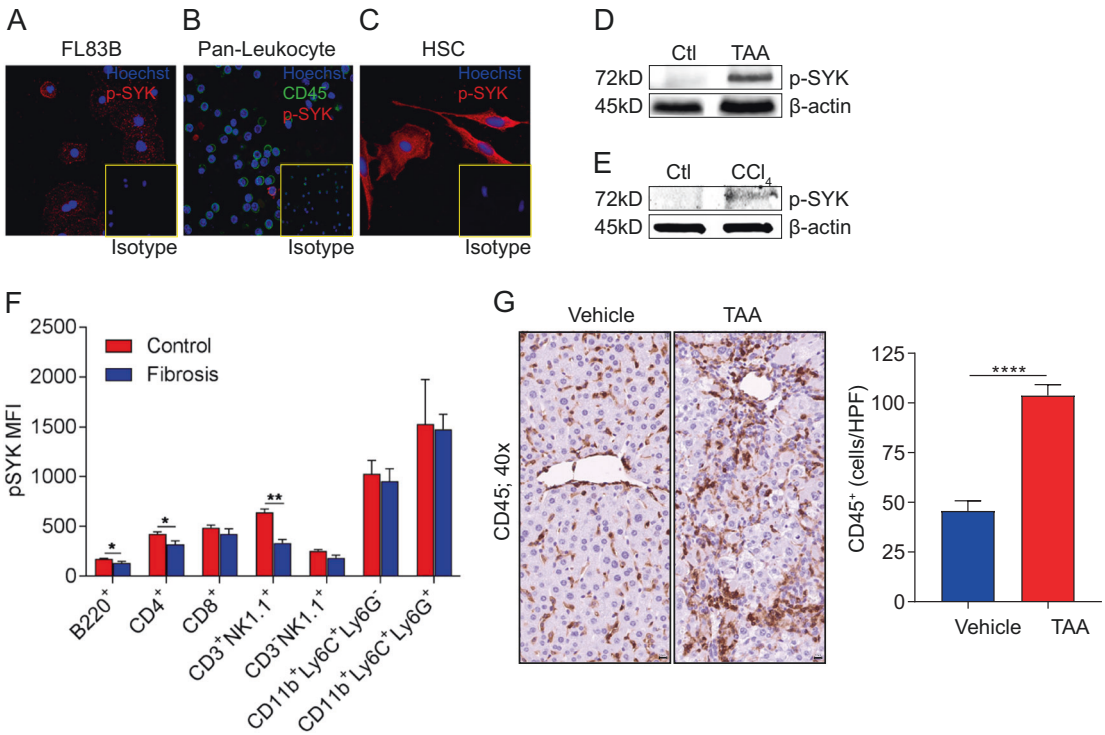

Fig. 1 p-SYK is expressed in liver fibrosis. **a** FL83B hepatocytes were stained with an Ab specific for p-SYK or isotype control. **b** Murine hepatic leukocyte were harvested and co-stained with Abs against CD45 and p-SYK or isotype control. **c** Primary murine hepatic stellate cells were stained with an Ab specific for p-SYK or isotype control. **d** C57BL/6 mice were serially injected with either PBS or TAA for 12 weeks ($n = 5$/group). Livers were probed for expression of p-SYK and β-actin by western blotting. **e** FL83B hepatocytes were treated with either PBS or CCL_4 and probed for expression of p-SYK and β-actin by western blotting. **f** C57BL/6 mice were serially injected with either PBS or TAA for 12 weeks ($n = 5$/group). Hepatic leukocytes were co-stained for p-SYK and CD45, CD3, CD4, CD8, NK1.1, CD11b, Ly6C, Ly6G, and B220. Groups were compared using the *t*-test. **g** C57BL/6 mice were serially injected with either PBS or TAA for 12 weeks ($n = 5$/group). Paraffin-embedded liver sections were tested for $CD45^+$ pan-leukocyte infiltration by IHC. Representative images and quantitative data are shown. Each experiment was repeat at least four times ($^*p < 0.05$; $^{**}p < 0.01$; $^{****}p < 0.0001$)

response to ligation of diverse pattern recognition receptors (PRRs) [9, 12]. We found that SYK inhibition dampens HSC activation in response to TLR4 ligation but does not mitigate HSC response to TLR9 or Dectin-1 ligation (Fig. 5d, e). Accordingly, the in vivo protection associated with SYK inhibition was TLR4 dependent (Fig. 5f). In aggregate, these data indicate that SYK signaling is necessary for robust HSC activation in vitro and response to select PRRs.

SYK inhibition rescues T cell loss and promotes $CD4^+$ T cell expression of protective cytokines in liver fibrosis

Since hepatic T cells modulate liver fibrosis [13], we postulated that SYK inhibition may alter the T cell phenotype in the fibrotic liver. We found that whereas the fraction of conventional $CD3^+NK1.1$- T cells were diminished in liver fibrosis in TAA-treated mice, SYK inhibition prevented diminution of the fraction of intra-hepatic conventional T cells (Fig. 6a). By contrast, targeting SYK only marginally restored $CD3^+NK1.1^+$ NKT cell numbers. Moreover, SYK inhibition in liver fibrosis upregulated hepatic $CD4^+$ T cells expression of the protective cytokines IFN-γ and IL-10 and reduced expression of the hepatotoxic cytokine TNF-α (Fig. 6b). Notably, a subset of $CD4^+$ T cells in the TAA + Piceatennol group exhibited a distinct IFN-γ^+IL-10^+ regulatory phenotype which was minimally-expressed in $CD4^+$ T cells in controls (Fig. 6c). Collectively, these data indicate that SYK inhibition reverses T cell loss and promotes $CD4^+$ T cell expression of protective cytokines in liver fibrosis.

SYK inhibition impedes B cells from adopting a pro-fibrotic phenotype

B cells expand in liver fibrosis and have been implicated in promoting disease progression [14]. B cell express comparatively low p-SYK in fibrotic liver compared to control liver (Fig. 1f). Nevertheless, we found that B cell expansion was dampened by SYK inhibition based on analyses by immunohistochemistry (Figure S2B) and flow cytometry (Fig. 6d). Further, examination of B cell subsets suggested that marginal zone B cells, which are associated with pro-inflammatory cytokine production, were expanded in the

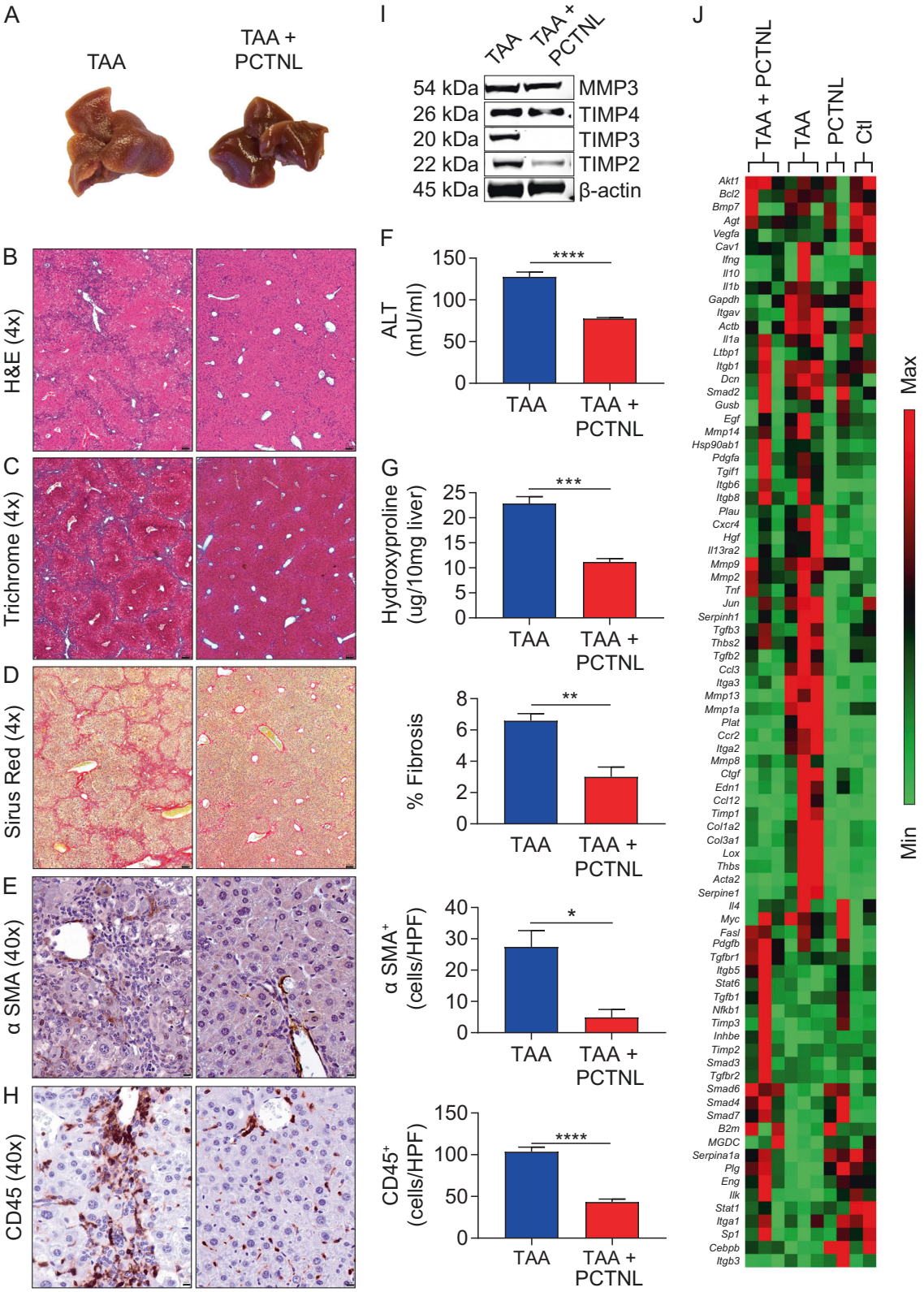

TAA-treated liver but were not expanded liver fibrosis in the context of SYK inhibition (Fig. 6e). Consistent with this observation, hepatic B cell expression of the hepato-protective cytokine IL-10 was reduced in liver fibrosis but remained at baseline levels in the TAA + Piceatannol cohort (Fig. 6f). Collectively, these data indicate that SYK

◀ **Fig. 2** SYK inhibition ameliorates liver fibrosis. **a**–**j** C57BL/6 mice were serially administered vehicle, Piceatannol, TAA, or TAA and Piceatannol for 12 weeks ($n = 5$/group). Livers were harvested and analyzed by (**a**) Gross appearance, (**b**) H&E, (**c**) Trichrome, (**d**) Sirius Red staining, and (**e**) α-SMA immunohistochemistry. **f** Serum ALT and (**g**) Hydroxyproline levels were quantified. Liver fibrosis as a percentage of total liver area was calculated based on Sirius Red staining. α-SMA staining was quantified. **h** Paraffin-embedded liver sections were tested for $CD45^+$ pan-leukocyte infiltration by IHC. Representative images and quantitative data are shown. **i** Livers were probed for expression of MMP3, TIMP4, TIMP3, TIMP2 and β-actin by western blotting. **j** Livers were tested for expression of fibrosis related genes using RT-PCR array. Each experiment was repeated at least 4 times using 5 mice per group (*$p < 0.05$; **$p < 0.01$; ***$p < 0.001$; ****$p < 0.0001$)

inhibition prevents hepatic B cells from adopting a pro-fibrotic phenotype.

SYK inhibition alters myeloid cell programming which regulates liver fibrosis

Besides affecting T and B cell differentiation, analysis of the $CD11b^+Ly6C^+Ly6G^-$ monocyte population in the fibrotic liver suggested that whereas inflammatory monocytes increased ~4-fold in TAA-treated mice, SYK inhibition completely blunted their cellular expansion (Fig. 7a). By contrast, $CD11b^+Ly6C^+Ly6G^+$ hepatic neutrophil populations were not expanded in fibrosis or affected by SYK inhibition. Moreover, SYK inhibition negated the upregulation of TNF-α in inflammatory monocytes (Fig. 7b).

Since we discovered that SYK is expressed in parenchymal and diverse inflammatory cells in the liver and inhibition of SYK signaling attenuates inflammation in both intra-hepatic T and B lymphocytes as well as in monocytes and HSC, we endeavored to determine the central compartment in which SYK signaling promotes hepatic fibrosis. We crossed $Syk^{fl/fl}$ mice with Alb^{Cre}, $Lrat^{Cre}$, $Cd4^{Cre}$, $Cd19^{Cre}$, and $LyzM^{Cre}$ mice to generate animals that are deficient in SYK signaling in hepatocytes, HSC, CD4 T cells, B cells, and myeloid cells, respectively. Targeting SYK in hepatocytes did not mitigate the severity of liver fibrosis. Similarly, targeting SYK in HSC, T cells, or B cells did not have protective effects. However, deletion of SYK in myeloid cells offered marked protection against liver fibrosis (Fig. 7c). To investigate the protective mechanism of targeting SYK signaling in myeloid cells, we used in vitro modeling. Monocytic bone marrow cultures were treated with vehicle or Piceatannol and assessed for effects on cellular differentiation. SYK inhibition reduced TNF-α expression but upregulated CD206 in myeloid cell cultures (Fig. 7d, e). Accordingly, monocytic bone marrow cultures derived from $LyzM^{Cre};Syk^{fl/fl}$ mice exhibited M2-like macrophage polarization (Fig. 7f). Collectively, these data indicate that inhibition of SYK signaling directs myeloid cell differentiation toward an anti-inflammatory phenotype.

To further investigate the influence of SYK signaling on myeloid cell programming, we analyzed changes in the global transcriptome in bone marrow-derived myeloid cells after treatment with Piceatannol or vehicle. SYK inhibition resulted in marked transcriptomic changes in myeloid cells (Fig. 8a, b). Gene ontology analysis suggested that targeting SYK signaling induced downregulation in inflammatory response (Fig. 8c). Ingenuity analysis demonstrated that pathways upregulated by Piceatannol included ERK5 and PPAR signaling whereas IL-8 and Oxidative phosphorylation were downregulated (Fig. 8d). Gene set enrichment analysis (GSEA) confirmed that genes linked to Oxidative phosphorylation were markedly reduced in myeloid cells in the context of SYK inhibition (Fig. 8e, f).

Discussion

Liver fibrosis is a scarring process following repeated hepatic injury and is the major risk factor for development of hepatocellular carcinoma. Patients suffering from liver fibrosis have no curative treatment options. It is well established that the innate immune system plays a central role in modulating the fibrosis-carcinogenesis axis [15, 16]. The liver is abundant with innate immune cells including macrophages, dendritic cells, neutrophils, inflammatory monocytes, NK cell, and NKT cells which serve to shape the response to fibrogenic injury [13, 17]. The gut microbiome critically modulates the phenotype these cells. Increased intestinal permeability associated with inflammatory disease leads to the portal venous translocation of intestine-derived bacterial byproducts to the liver, including lipopolysaccharide (LPS) and unmethylated CpG motifs [18]. These gut-derived bacterial products stimulate an array of TLRs, which are expressed on diverse innate immune cells as well as on endothelial cells, biliary epithelial cells, hepatic stellate cells, and hepatocytes. TLR signaling activates these cells and contributes to a cycle of inflammation that eventuates in liver parenchymal scarring and neoplastic transformation [19, 20]. In the current study, we discovered robust SYK expression in both the liver parenchymal and immune compartments. We found that SYK inhibition prevented the pathogenic activation of myeloid cells, B cells, and T cells. Inhibition of SYK also mitigated HSC transdifferentiation. Moreover, pharmacologically targeting was SYK protective against liver fibrosis and cancer development. We used 2 inhibitors in our study, Piceatannol and PRT062607. The latter achieves complete inhibition of SYK signaling and is considered to be more selective [21]. Our results are consistent with a recent report that found that delivery of SYK inhibitor using PLGA nanoparticles can be

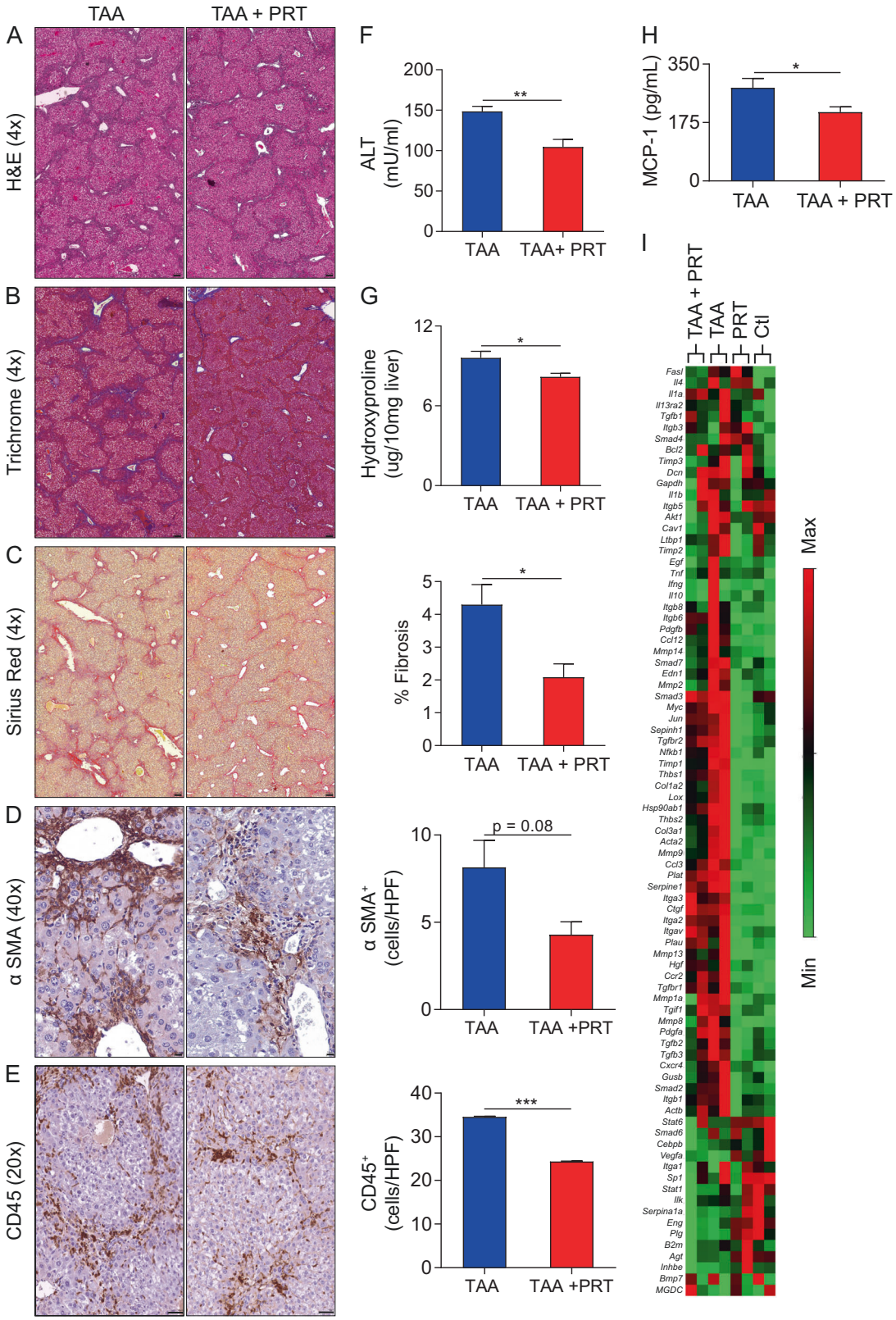

a potential therapeutic approach for the treatment of non-alcoholic steatohepatitis [22]. Our work is also consistent with another report that found that SYK upregulation in HSC promoted their activation by increasing expression of diverse fate determining transcription factors including MYB proto-oncogene transcription factor (MYB), CREB

◀ **Fig. 3** p-SYK inhibition protects against liver fibrosis. **a–i** C57BL/6 mice were serially given either vehicle, PRT, TAA or TAA + PRT for 12 weeks ($n = 5$/group). Livers were harvested and analyzed by (**a**) H&E, (**b**) Trichrome, and (**c**) Sirius Red staining, (**d**) α-SMA IHC, and (**e**) CD45 IHC. Liver fibrosis as a percentage of total liver area was calculated based on Sirius Red staining and α-SMA and CD45 staining were quantified. **f** Serum ALT and (**g**) Hydroxyproline levels were quantified. (**h**) Serum level of MCP-1 was measured in a cytometric bead array. **i** Livers were tested for expression of fibrosis-related genes using RT-PCR array. Each experiment was repeat at least 3 times using 5 mice per group ($*p < 0.05$; $**p < 0.01$; $***p < 0.0001$)

binding protein and MYC proto-oncogene (MYC) [10]. Of note, HBV and HCV infection, which are primary risk factors for and drivers of malignant transformation, significantly increased both SYK expression in hepatic parenchymal cells and fibrosis-related gene transcription in HSC [10]. However, our targeted in vivo deletion experiments suggested that only SYK inhibition in myeloid cells was critical to fibrogenic progression. By contrast, whereas deletion of SYK in T cells, B cells, HSC, or hepatocytes mitigated the inflammatory phenotype of these cells, it did not influence the resultant liver fibrosis.

We found that SYK inhibition reprograms monocytic bone marrow cells towards an alternatively activated $TNF\alpha^{low}$ phenotype. This contrasts with our previous finding in the context of the pancreatic cancer tumor microenvironment that activation of Dectin-1, which signals via SYK, has immune-suppressive effects on the polarization of macrophages and monocytic cells [23]. However, whereas the pancreas and liver are similar in that inflammation, fibrosis, and oncogenesis are intrinsically linked, SYK signaling may have distinct effects in the liver than from the pancreas. Indeed, we have shown that pancreatic cancer has a uniquely tolerogenic inflammatory milieu which differs from most other contexts. For example, inhibition of MyD88 which effectively abrogates nearly all TLR signaling exacerbates pancreatic inflammation, fibrosis, and oncogenesis [24]. By contrast, targeting MyD88 is protective against hepatic fibrosis and liver cancer [25, 26]. Moreover, the physiologic and oncogenic consequences of directly targeting SYK, which controls a diversity of signaling mechanisms, versus specifically targeting Dectin-1, may differ. For example, contrary to the current observations directly targeting SYK, we previously reported that Dectin-1 signaling is protective against liver fibrosis [9]. We found that Dectin-1 inhibits TLR4 signaling by mitigating TLR4 and CD14 expression, each of which are regulated by Dectin-1-dependent M-CSF expression. Notably, the mechanism by which targeting SYK influences myeloid cell inflammatory phenotype was addressed by our RNAseq experiments and suggested that whereas targeting SYK upregulates IL-8, it downregulates ERK5, PPAR, mTOR, and oxidative phosphorylation signaling. Oxidative phosphorylation is linked to cellular metabolism in leukocytes which is correlated with pro-inflammatory cellular function [27]. Our data suggest that the anti-oxidative capacity of monocytic cells may reduce liver damage and subsequently inhibit liver fibrosis. Oxidative phosphorylation has not been intensively studied in inflammatory cells in liver fibrosis and liver cancer and the consequences of oxidative phosphorylation in directly affecting monocytic cells in the liver when targeting SYK requires more exact study.

An important observation in the current study is that anti-fibrogenic effect of SYK inhibition is TLR4-dependent. TLR4 signaling is a driver of HSC activation and fibrosis progression. Elevation in LPS and TLR4 activation have been well-documented both in experimental animal models and in patients with end-stage liver diseases [28]. TLR4 signaling promotes HSCs activation to TGF-β in an NF-κB-dependent manner, which leads to the accumulation of both inflammatory and resident macrophages to the damaged site [29]. TLR4 activation has been linked to hepatocarcinogenesis via its activation by LPS which is produced by distinct pathogenic strains of *E. coli* [30]. Epiregulin is a TLR4-regulated hepatomitogen that also promotes hepatocarcinogenesis [30]. Moreover, the interface of SYK and TLR4 signaling pathways has been previously reported in diverse myeloid cells [31]. In the current study, we found that targeting SYK dampens HSC activation in response to TLR4 ligation. Moreover, SYK inhibition offers protection only in the context of intact TLR4 signaling suggesting that SYK and TLR4 appear to have overlapping pro-fibrinogenic mechanisms.

The clinical and therapeutic implications of our findings for hepatocellular carcinoma treatment are important. Sorafenib and other new generation tyrosine kinase inhibitors have shown modest efficacy in clinical trials and are currently first line treatment for advanced hepatocellular carcinoma that are not amenable to surgical or loco-regional therapies [32]. Patients treated with Sorafenib had a 3-month survival advantage over those treated with best supportive care [33]. Further, immunotherapy has recently emerged as an efficacious treatment modality for liver cancer and αPD1 based regimens are now FDA approved as second line therapy for patients with advanced hepatocellular carcinoma that have failed therapy with tyrosine kinase inhibitors as response rates to αPD-1 mAbs have approached 20% [34]. Our data is based on models of cancer prevention. Further studies are necessary to determine whether the development of clinical SYK inhibitors may be an attractive strategy in experimental oncologic therapy of liver cancer and may ultimately offer additional therapeutic options for patients with established liver cancer.

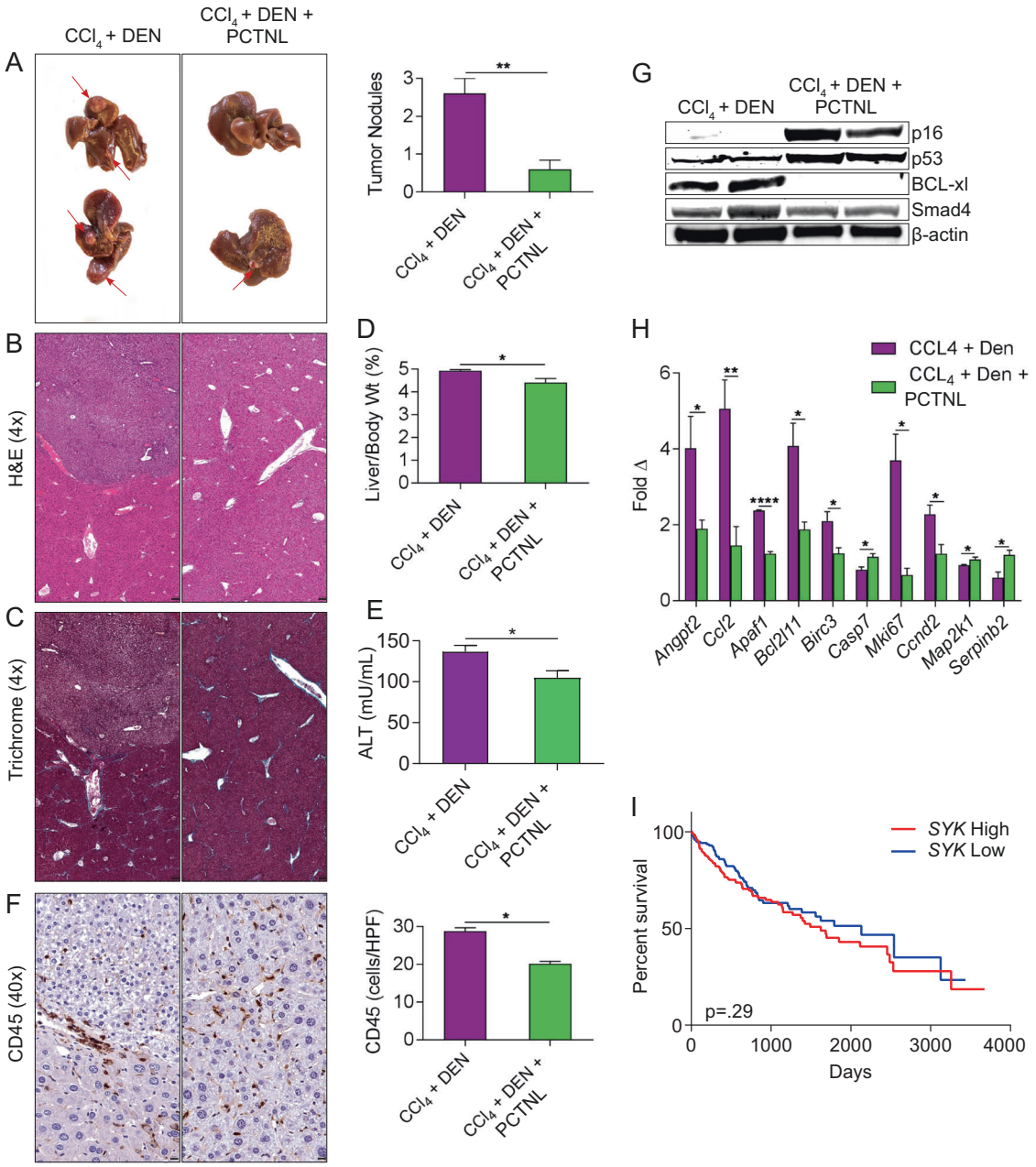

Fig. 4 p-SYK inhibition protects against hepatocellular carcinoma. **a**–**h** Mice were treated with CCl_4 + DEN or CCl_4 + DEN + Piceatannol. **a** Representative gross images of livers are shown and number of visible tumor nodules were quantified. **b** Representative H&E-stained paraffin-embedded liver sections are shown. **c** Representative Trichrome-stained paraffin-embedded liver sections are shown. **d** Liver weight/body weight ratio was calculated. **e** Serum ALT was measured. **f** $CD45^+$ pan-leukocyte infiltration was determined by IHC. Representative images and quantitative data are shown. **g** Liver tissues were assessed by western blotting for expression of p16, p53, BCL-xl, Smad4, and β-actin. **h** Liver tissues were assessed by RT-PCR for select oncogenic genes. **i** Ten-year Kaplan-Meier survival curve of human liver cancer patients stratified by high ($n = 188$) versus low ($n = 177$) *SYK* expression based on TCGA data. (*$p < 0.05$; **$p < 0.01$; ****$p < 0.0001$)

Materials and methods

Animals and in vivo models

C57BL/6 J, $Tlr4^{-/-}$, $Syk^{fl/fl}$, Alb^{Cre}, $Cd4^{Cre}$, $LyzM^{Cre}$ and $Cd19^{Cre}$ mice were purchased from Jackson Labs (Bar Harbor, ME). $Lrat^{Cre}$ mice were a gift of Robert Schwabe (Columbia University, NY). Animals were bred in-house and housed in a clean vivarium. To induce hepatic fibrosis, 12-week-old female mice were treated with thrice weekly injections of thioacetamide (TAA) (250 mg/kg; Alfa Aesar, Haverhill, MA) for 12 weeks as we previously reported [9].

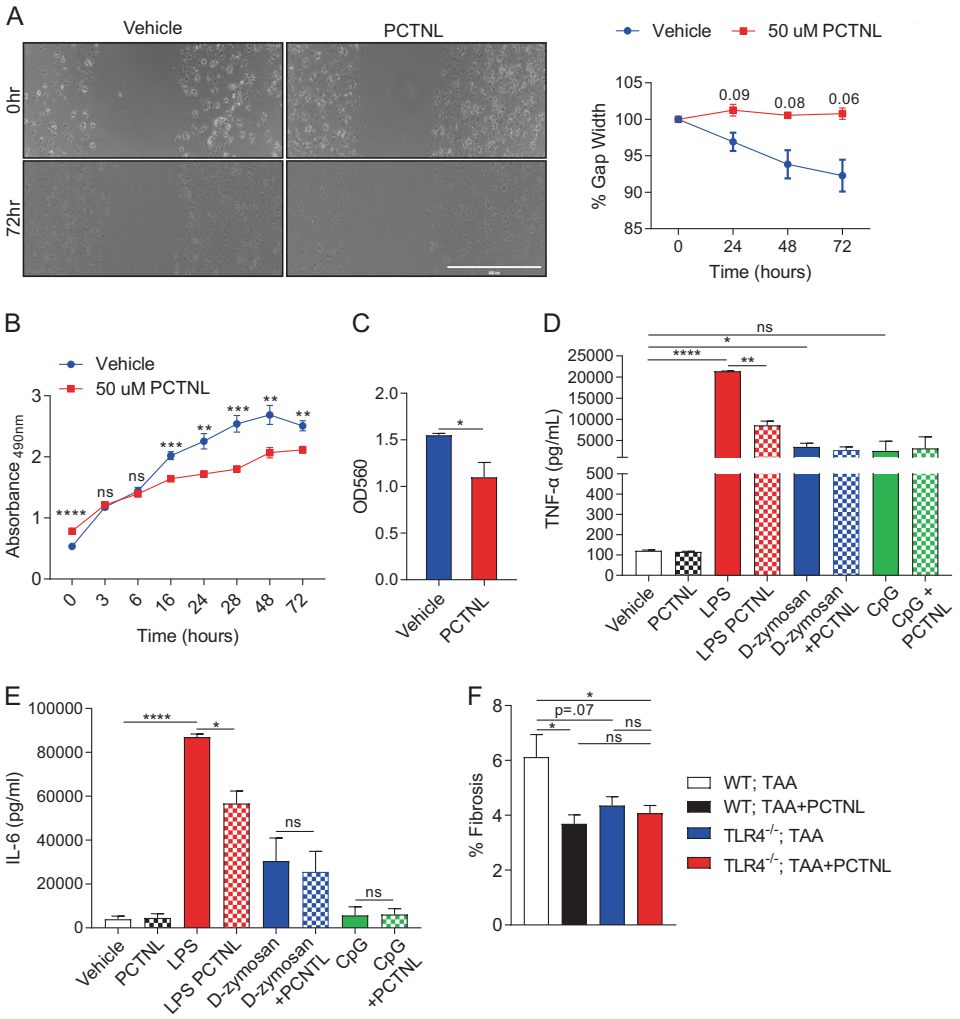

Fig. 5 SYK inhibition mitigates HSC activation and response to TLR4 ligation. **a** HSC cellular migration after treatment with vehicle or Piceatannol was determined over 72 h in a scratch assay. Representative images and quantitative data are shown. This experiment was performed in triplicate and repeated twice. **b** HSC cellular proliferation after treatment with vehicle or Piceatannol was determined over 72 h in an XTT assay. This experiment was performed in triplicate and repeated three times. **c** HSC mobilization after treatment with vehicle or Piceatannol was measured in a transwell assay. This experiment was performed in quadruplicate and repeated twice. **d**, **e** HSC were treated with TLR4 (LPS), TLR9 (CpG), or Dectin-1 (D-Zymosan) ligands in combination with vehicle or Piceatannol. Concentration of (**d**) TNF-α and (**e**) IL-6 in the supernatant were determined at 24 h. This experiment was performed in quadruplicate and repeated twice. **f** WT and TLR4$^{-/-}$ mice were serially administered TAA or TAA and Piceatannol for 12 weeks ($n = 5$/group). Livers were harvested and analyzed for fibrosis by Sirius Red staining (*$p < 0.05$; **$p < 0.01$; ***$p < 0.001$; ****$p < 0.0001$)

To induce HCC, 2-week-old male mice were administered with a single dose of DEN (15 mg/kg; Sigma-Aldrich, Saint Louis, MO) via i.p. injection followed by bi-weekly injections of CCl_4 (0.2 ml/kg; Sigma-Aldrich) starting at 8 weeks of age, and mice were sacrificed 24 weeks later [30]. In select experiments, mice were treated with thrice weekly with Piceatannol (20 mg/kg; Selleckchem; Houston, TX) or corn oil via oral gavage for 12 weeks. All studies were approved by the Institutional Animal Care and Use Committee (IACUC) at NYU School of Medicine. Experiments were conducted in accordance with the NYU School of Medicine policies on the care, welfare, and treatment of laboratory animals.

Cellular isolation

Murine hepatic non-parenchymal cells (NPC) were collected as previously described [9]. Mice weighing 18–22 g were anesthetized and the portal vein was cannulated. First, the liver was perfused with an EGTA solution (containing 5.4 mmol/L KCl, 0.44 mmol/L KH_2PO_4, 140 mmol/L NaCl, 0.34 mmol/L Na_2HPO_4, 0.5 mmol/L EGTA, and 25 mmol/L Tricine, pH 7.2); and then with Gey's Balanced Salt Solution (GBSS) containing 0.075% type I collagenase (Sigma-Aldrich), followed by additional digestion step (0.009% collagenase at 37 °C with agitation and incubation for 15 min). Hepatocytes were separated with 25 × *g* centrifugation for 5 mins at room temperature as described previously [35]. To further isolate hepatic stellate cell, the supernatant was centrifuged at 400 × *g* for 10 mins at 4 °C. The cell pellet was suspended in 11.5% OptiPrep and loaded carefully with GBSS. After centrifugation at 1400 × *g* for 20 mins at 4 °C, the interface fraction was collected and further washed with GBSS twice. Collected HSCs were cultured further in RPMI-1640 medium containing 10% FBS and 10% horse serum as previously reported [36]. FL83B hepatocyte cells were obtained from ATCC (CRL-2390).

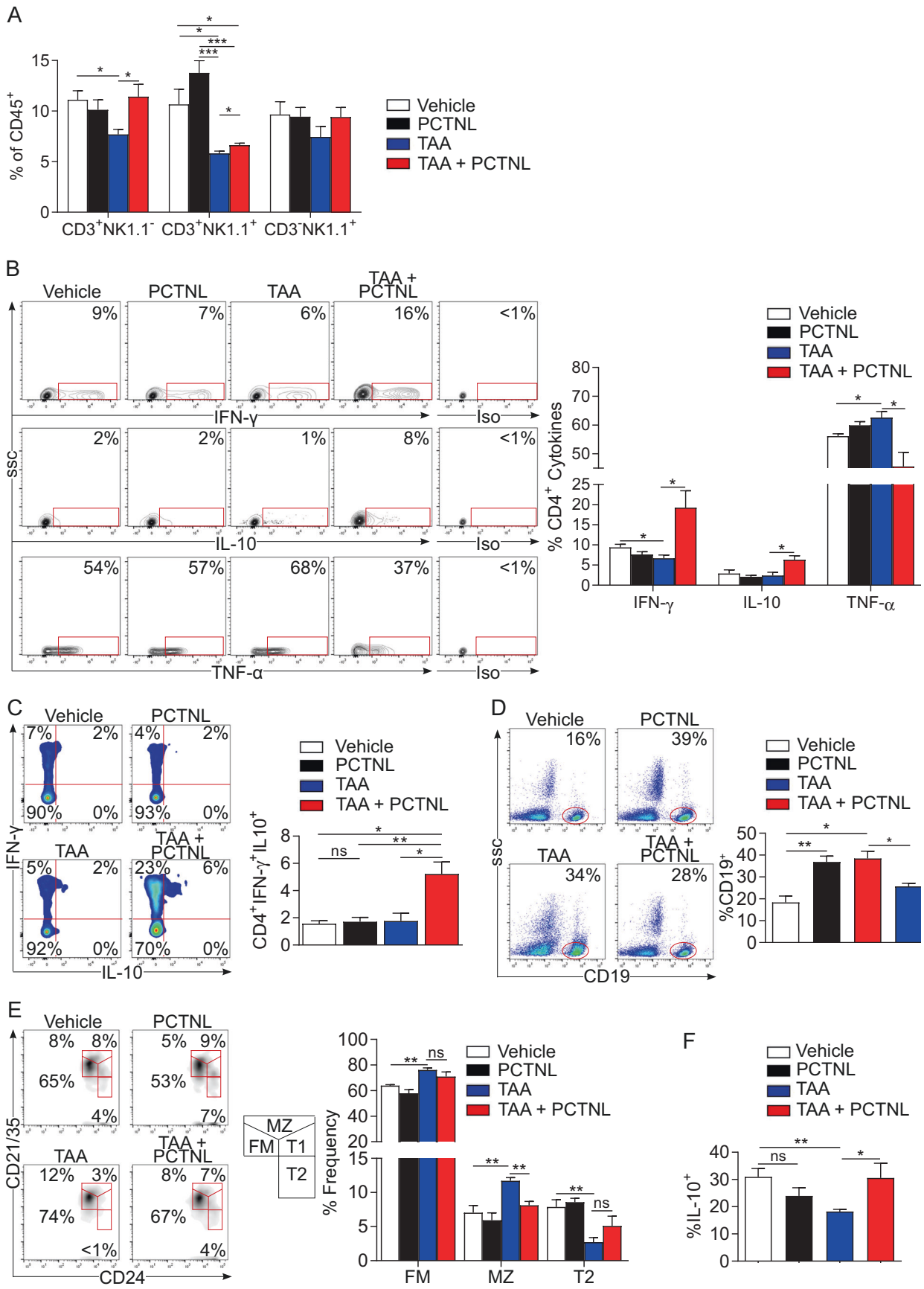
A
% of CD45+
CD3+NK1.1- CD3+NK1.1+ CD3-NK1.1+
Vehicle
PCTNL
TAA
TAA + PCTNL
B
Vehicle
PCTNL
TAA
TAA + PCTNL
IFN-γ
IL-10
TNF-α
Iso
ssc
% CD4+ Cytokines
C
IFN-γ
IL-10
CD4+IFN-γ+IL10+
D
ssc
CD19
%CD19+
E
CD21/35
CD24
MZ
FM
T1
T2
% Frequency
F
%IL-10+
ns

◀ **Fig. 6** SYK inhibition modulates intrahepatic immune phenotype. **a** Hepatic non-parenchymal cells (NPC) from livers mice treated with vehicle, TAA, Piceatannol, or TAA + Piceatannol were co-stained using Abs against CD45, CD3 and NK1.1. Quantitative data are shown. **b** $CD4^+$ T cells from livers of control mice or mice treated with vehicle, TAA, Piceatannol, or TAA + Piceatannol were gated and tested for expression of IFN-γ, IL-10, and TNF-α. Representative contour plots and quantitative data are shown. **c** $CD4^+$ T cells from livers of control mice or mice treated with vehicle, TAA, Piceatannol, or TAA + Piceatannol were gated and tested for co-expression of IFN-γ and IL-10. Representative and quantitative data are shown. **d** C57BL/6 mice were serially administered vehicle alone, Piceatannol alone, TAA alone, or TAA and Piceatannol for 12 weeks ($n = 5$/group). Livers were harvested and $CD45^+$ NPC were stained for $CD19^+$ B cells. Representative dot plots and quantitative data are shown. **e** $CD19^+IgM^+$ B cells were gated and analyzed for co-expression of CD24 and CD21/35. The gating strategy and fraction of FM, MZ, T2, and T1 B cells are shown. **f** B cell expression of IL-10 was determined. Representative dot plots and quantitative data are shown (*$p < 0.05$; **$p < 0.01$; ***$p < 0.001$)

Flow cytometry

For flow cytometry, single-cell suspensions of NPC were incubated with Zombie Yellow (BioLegend, San Diego, CA) for 10 min, followed by Fc blocking reagent (Biolegend, San Diego, CA) for 10 mins and a 30-min incubation with fluorescently-conjugated mAbs directed against mouse CD45 (30-F11), CD3 (17A2), B220 (RA3-6B2), CD19 (6D5), CD4 (GK1.5), CD8 (53-6.7), Ly6C (HK1.4), Ly6G (1A8), NK1.1 (PK136), CD11b (M1/70), F4/80 (BM8), CD206 (C068C2), CD21/35 (7E9), or CD24 (M1/69) (all BioLegend, San Diego, CA). For intracellular cytokine staining, cells were incubated for 4–6 h in complete media (RPMI 1640 with 10% heat-inactivated FBS, 2 mM L-glutamine, 100 U/ml penicillin, 100 µg/ml streptomycin, non-essential amino acids, 1 mM sodium pyruvate, 25 mM HEPES, and 0.05 mM β-ME) and stimulated by cell stimulation cocktail plus protein transport inhibitors (500×; eBioscience, San Diego, CA). After stimulation, cells were washed, fixed and permeabilized using Fixation/Permeabilization kit (BD Biosciences, Franklin Lakes, NJ) and subsequently stained with fluorescently conjugated IFN-γ (XMG1.2), IL-10 (JES5-16E3), and TNF-α (MP6-XT22), (all Biolegend, San Diego, CA). Experiments were performed using the LSRII (BD Biosciences) and analyzed using FlowJo software (Tree Star, Ashland, OR).

Histopathology, immunohistochemistry and microscopy

For histological analysis, liver specimens were fixed with 10% buffered formalin, dehydrated in ethanol, and then embedded with paraffin, and stained with hematoxylin-eosin (H&E), Sirius Red and Gomori Trichrome. The percentage of fibrosis were calculated, as previously described [37]. For immunohistochemical analysis, formalin fixed paraffin embedded slides were stained for anti-mouse CD45 (30-F11), CD45R/B220 (RA3-6B2; both BD Biosciences), MPO (ab9535), CD68 (ab5690), and α-SMA (ab5694; all Abcam, Cambridge, MA). Light microscopic images were captured with a Zeiss Axioscope 40 microscope/camera system (Zeiss, Thornwood, NY). Cell count was quantified by examining 10 high powered fields (HPFs) per slide. Immunofluorescent images were acquired using a Zeiss LSM700 confocal microscope with ZEN 2010 software (Carl Zeiss, Thornwood, NY).

HSC experiments

For cellular proliferation assays, 2×10^3 HSCs were seeded and incubated in 96-well plates. HSC proliferation was measured using the XTT assay kit according to the manufacturer's protocol (Sigma-Aldrich). For cell migration assays, 3×10^3 HSCs were seeded in the upper compartment of a 8 µm Transwell chambers in 24 well plates (Corning, Teterboro, NJ) and were cultured with FBS-free RPMI, while the lower compartment was filled with complete medium containing DMSO or Piceatannol (50 µM). Cell migration was determined following manufacturer's instructions. For scratch assays, 5×10^5 HSCs were seeded and maintained in 6-well plates for a week, a scratch was made and HSCs were treated in 2 mL complete RPMI medium with DMSO or Piceatannol (50 µM). Gap width was determined at different time points. In select experiments HSCs were treated with TLR4 ligand (LPS, 1 µg/ml), TLR9 ligand (CpG ODN 1826, 5 µM) and Dectin-1ligand (Depleted Zymosan, 1 µg/ml; all Invivogen, San Diego, CA).

Western blotting, PCR, and biochemical assays

For Western blotting, total protein was isolated from 10 mg liver tissue by homogenization in RIPA buffer (50 mM pH 7.4 Tris-Hcl, 150 mM NaCl, 0.5% Na-deoxycolate, 0.5% NP-40, 0.25% SDS, 5 mM EDTA) with Complete Protease Inhibitor cocktail (Roche, Pleasanton, CA). Proteins were separated from larger fragments by centrifugation at $14{,}000 \times g$. After determining total protein by Bradford protein assay, 10% polyacrylamide gels (NuPage, Invitrogen, Grand Island, NY) were equiloaded, electrophoresed at 200 V, electrotransferred to PVDF membranes, and probed with mAbs to p16, p53, Bcl-xL, Smad4, p-SYK, MMP3, TIMP2, TIMP3, TIMP4, and β-actin (all Abcam). Blots were developed using Li-Cor (Li-Cor Biosciences, Lincoln, NE). Total RNA was extracted using an RNeasy mini kit (Qiagen, Valencia, CA) and cDNA was synthesized using the High-Capacity cDNA Reverse Transcription Kit (Applied Biosystems, Foster City, CA). Total liver or liver

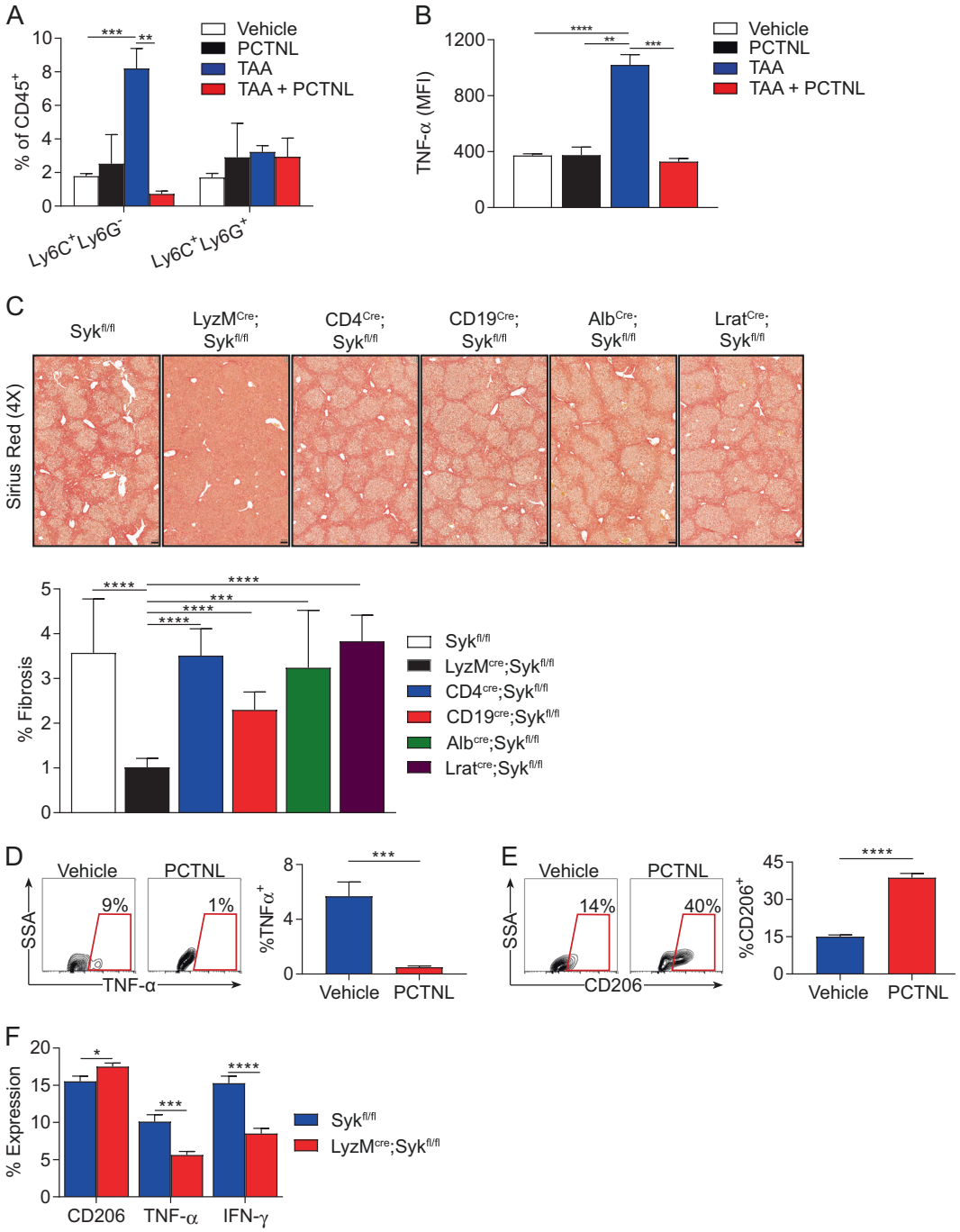

Fig. 7 Compartment-specific deletion of SYK indicates critical role for myeloid cells. **a** CD11b^{+} hepatic leukocytes from livers of control mice or mice treated with vehicle, TAA, Piceatannol, or TAA + Piceatannol were co-stained using Abs against Ly6G and Ly6C and analyzed by flow cytometry. **b** CD11b^{+}Ly6C^{+}Ly6G^{-} inflammatory monocytes from livers of control mice or mice treated with vehicle, TAA, Piceatannol, or TAA + Piceatannol were gated and tested for co-expression of TNF-α. Representative histograms and quantitative data are shown. Each experiment was performed 3 times using 5 mice per group. **c** Littermate *Syk$^{fl/fl}$*, *LyzM^{Cre};Syk$^{fl/fl}$*, *Cd4^{Cre};Syk$^{fl/fl}$*, *Cd19^{Cre};Syk$^{fl/fl}$*, *Alb^{Cre};Syk$^{fl/fl}$*, and *Lrat^{Cre};Syk$^{fl/fl}$* mice were serially administered TAA for 12 weeks. Livers were harvested and analyzed by Sirius Red staining. Representative images are shown and liver fibrosis as a percentage of total liver area was calculated. This experiment was repeated twice with similar results. **d**, **e** Monocytic bone marrow cultures were treated with vehicle or Piceatannol and assessed for expression of (**d**) TNF-α and (**e**) CD206. **f** Monocytic bone marrow cultures derived from *LyzM^{Cre};Syk$^{fl/fl}$* mice and littermate controls were tested for expressions of CD206, TNF-α and IFN-γ (n = 11/12 replicates/group; $^{**}p < 0.01$; $^{***}p < 0.001$; $^{****}p < 0.0001$)

tumor RNA was assayed using a PCR Array for liver fibrosis (PAMM-120ZA) and Oncogenes & Tumor Suppressor Genes (PAMM-502Z) as per the manufacturer's protocol. Serum ALT level was tested with a Colorimetric

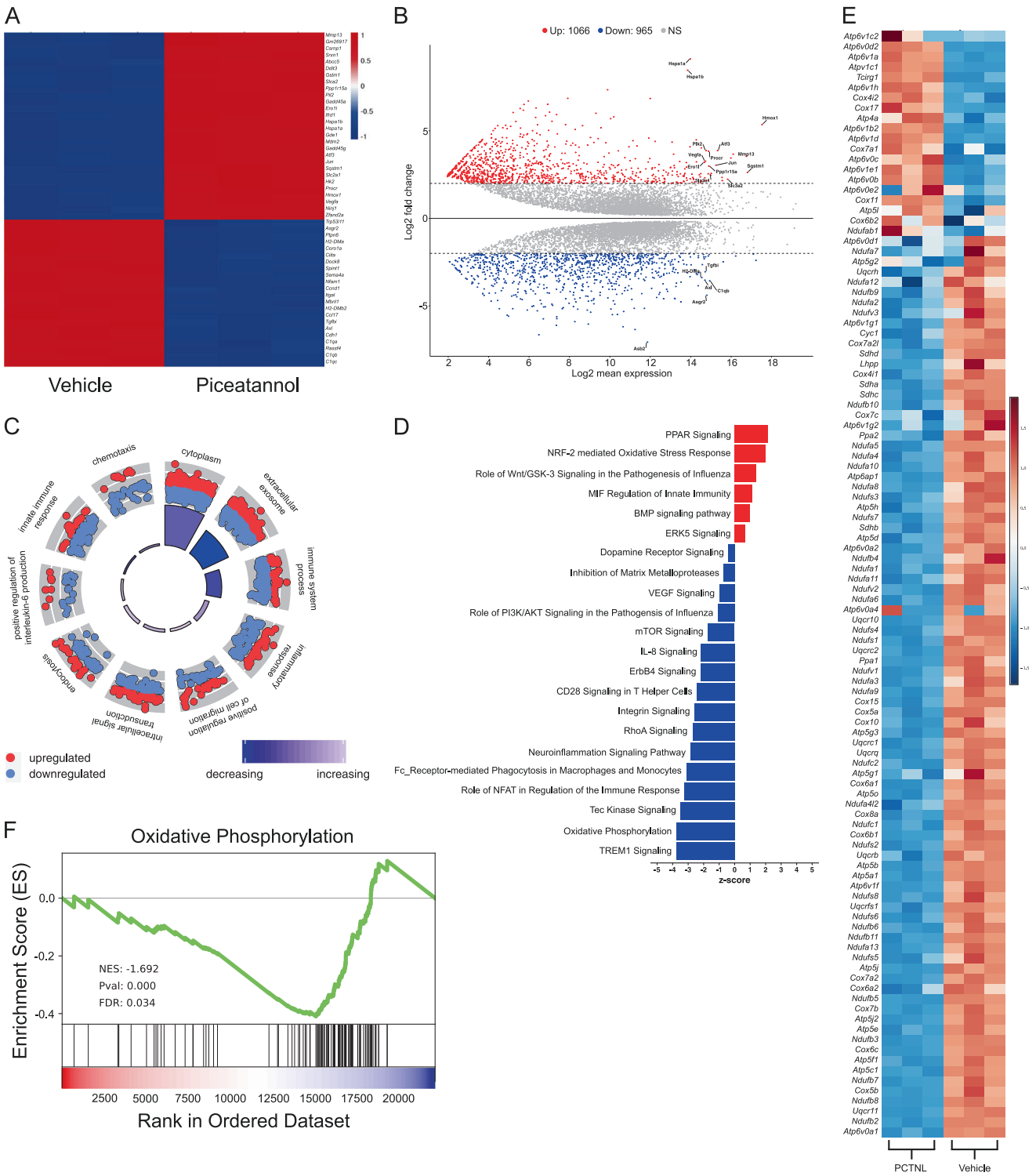

Fig. 8 Transcriptomic analysis of myeloid cells treated with SYK inhibitor. **a**–**f** RNA-Seq analysis of myeloid cell cultures treated with vehicle or Piceatannol for 18 h ($n = 3$/group). **a** A heat map depicting the 50 most differentially expressed genes and (**b**) an MA plot showing global differential gene expression in the vehicle and Piceatannol treated cells are shown. **c** Top scoring Gene Ontology (GO) terms are shown in the circle plot. Red (up-regulated) and blue (down-regulated) dots in outer circle show the log2FC of genes in each GO term. Bar plot colors in the inner circle are based on z-scores, and the height of each bar represents each GO term's significance. **d** Ingenuity pathway analysis was performed and top ranking upregulated and downregulated pathways by z-score are shown. **e** A heat map depicting expression of oxidative phosphorylation related genes and (**f**) GSEA for oxidative phosphorylation is shown

Activity Assay Kit (#K752) and hepatic hydroxyproline was measured using a bioassay kit (# K555; both Biovision, Milpitas, CA) following the manufacturer's instructions.

RNA-Seq and analysis

RNA-Seq libraries were prepared using the Illumina TruSeq Stranded Total RNA library prep, after ribodepletion with Ribozero Gold kit (cat# 20020597, Illumina, San Diego, CA) starting from 500 ng of DNase I treated total RNA, following the manufacturer's protocol, with the exception that 9 cycles of PCR were performed to amplify the libraries. The amplified libraries were purified using AMPure beads, quantified by Qubit and qPCR, and visualized in an Agilent Bioanalyzer (Agilent, Santa Clara, CA). The libraries were pooled equimolarly and sequenced on one lane of an Illumina HiSeq 2500 flow cell, v4 chemistry as paired end 50. The raw fastq reads were aligned to mm10 mouse reference genome using STAR aligner [38]. Fastq Screen was used to check for any contaminations in the samples and Picard RnaSeqMetrics was used to obtain the metrics of all aligned RNA-Seq reads. *featureCounts* was used to quantify the gene expression levels [39]. The raw gene counts data were used for further differential expression analysis. To identify the differentially expressed genes, *DESeq2* R package was used [40]. The resulting genes with adjusted $p < 0.05$ were considered significant. Heatmaps were generated using *pheatmap* R package. To determine the functional annotation of the significantly expressed genes, Gene Ontology (GO) analysis was performed and the expression levels of genes in each term were represented in a GO circle plot using the R package *GOplot*. To identify the signaling pathways in which the genes are enriched, Ingenuity Pathway Analysis (IPA) was carried out for genes that were considered significant. The canonical pathways from IPA analysis were represented as a barplot and the regulatory network of genes represented using Cytoscape [41]. GSEA was performed on differentially expressed genes. Upregulated and downregulated sets of genes were ranked based on their average and normazlied log2 fold change between treatment and control group and each gene set was assessed for enrichment in the KEGG_2016 geneset library [http://amp.pharm.mssm.edu/Enrichr/#stats] using python package gseapy [https://pypi.org/project/gseapy/] for analyses. The GEO accession number is GSE125157.

Statistical analysis

Data is presented as mean ± standard error of mean. Statistical significance was determined by the Student's *t* test and the log-rank test using GraphPad Prism 7 (GraphPad Software, La Jolla, CA). *p*-values < 0.05 were considered significant. Significance for GSEA analysis was determined using the Wilcoxon rank sum test with Bonferroni multiple-comparison correction. Data on gene expression in human tissues was derived from the TCGA database (https://portal.gdc.cancer.gov/). Survival was measured by the Kaplan-Meier method and was analyzed by log-rank test.

Acknowledgements We thank the NYU Langone Health Genome Technology Center (GTC) for expert library preparation and sequencing; the GTC is partially supported by the Cancer Center Support Grant P30CA016087 at the Laura and Isaac Perlmutter Cancer Center. We thank the NYU Langone Health Experimental Pathology Research Laboratory, which is partially funded by NYU Cancer Institute Center Support Grant NIH/NCI 5 P30CA16087, for expert tissue processing and equipment support. This work was supported by NCI CA168611 (GM), CA155649 (GM), CA193111 (ATH, BD), Society of University Surgeons—Ethicon Resident Research Award (ATH), American Liver Foundation—Thomas F. Nealon, III Postdoctoral Research Fellowship Honoring Zachery Rue (ATH), American Liver Foundation Postdoctoral Research Fellowship (WW), NYU Physician-Scientist Training Program (ATH).

Compliance with ethical standards

Conflict of interest The authors declare that they have no conflict of interest.

References

1. Anderson RN, Smith BL. Deaths: leading causes for 2002. Natl Vital Stat Rep. 2005;53:1–89.
2. Poynard T, Mathurin P, Lai CL, Guyader D, Poupon R, Tainturier MH, et al. A comparison of fibrosis progression in chronic liver diseases. J Hepatol. 2003;38:257–65.
3. Moreira RK. Hepatic stellate cells and liver fibrosis. Arch Pathol Lab Med. 2007;131:1728–34.
4. Melhem A, Muhanna N, Bishara A, Alvarez CE, Ilan Y, Bishara T, et al. Anti-fibrotic activity of NK cells in experimental liver injury through killing of activated HSC. J Hepatol. 2006; 45:60–71.
5. Hellerbrand C, Stefanovic B, Giordano F, Burchardt ER, Brenner DA. The role of TGFbeta1 in initiating hepatic stellate cell activation in vivo. J Hepatol. 1999;30:77–87.
6. Pradere JP, Kluwe J, De Minicis S, Jiao JJ, Gwak GY, Dapito DH, et al. Hepatic macrophages but not dendritic cells contribute to liver fibrosis by promoting the survival of activated hepatic stellate cells in mice. Hepatology. 2013;58:1461–73.
7. Mocsai A, Ruland J, Tybulewicz VL. The SYK tyrosine kinase: a crucial player in diverse biological functions. Nat Rev Immunol. 2010;10:387–402.
8. Cornall RJ, Cheng AM, Pawson T, Goodnow CC. Role of Syk in B-cell development and antigen-receptor signaling. Proc Natl Acad Sci USA. 2000;97:1713–8.
9. Seifert L, Deutsch M, Alothman S, Alqunaibit D, Werba G, Pansari M, et al. Dectin-1 regulates hepatic fibrosis and hepatocarcinogenesis by suppressing TLR4 signaling pathways. Cell Rep. 2015;13:1909–21.
10. Qu C, Zheng D, Li S, Liu Y, Lidofsky A, Holmes JA et al. Tyrosine kinase SYK is a potential therapeutic target for liver fibrosis. Hepatology. 2018; https://doi.org/10.1002/hep.29881.

11. Uehara T, Pogribny IP, Rusyn I. The DEN and CCl4-induced mouse model of fibrosis and inflammation-associated hepatocellular carcinoma. Curr Protoc Pharmacol. 2014;66:14 30 11–10.
12. Weiskirchen R, Tacke F. Cellular and molecular functions of hepatic stellate cells in inflammatory responses and liver immunology. Hepatobiliary Surg Nutr. 2014;3:344–63.
13. Koyama Y, Brenner DA. Liver inflammation and fibrosis. J Clin Invest. 2017;127:55–64.
14. Novobrantseva TI, Majeau GR, Amatucci A, Kogan S, Brenner I, Casola S, et al. Attenuated liver fibrosis in the absence of B cells. J Clin Invest. 2005;115:3072–82.
15. Marcus A, Gowen BG, Thompson TW, Iannello A, Ardolino M, Deng W, et al. Recognition of tumors by the innate immune system and natural killer cells. Adv Immunol. 2014;122:91–128.
16. Wick G, Backovic A, Rabensteiner E, Plank N, Schwentner C, Sgonc R. The immunology of fibrosis: innate and adaptive responses. Trends Immunol. 2010;31:110–9.
17. Notas G, Kisseleva T, Brenner D. NK and NKT cells in liver injury and fibrosis. Clin Immunol. 2009;130:16–26.
18. Kant R, de Vos WM, Palva A, Satokari R. Immunostimulatory CpG motifs in the genomes of gut bacteria and their role in human health and disease. J Med Microbiol. 2014;63:293–308.
19. Yang J, Li M, Zheng QC. Emerging role of toll-like receptor 4 in hepatocellular carcinoma. J Hepatocell Carcinoma. 2015;2:11–17.
20. Yang L, Seki E. Toll-like receptors in liver fibrosis: cellular crosstalk and mechanisms. Front Physiol. 2012;3:138.
21. Coffey G, Rani A, Betz A, Pak Y, Haberstock-Debic H, Pandey A, et al. PRT062607 achieves complete inhibition of the spleen tyrosine kinase at tolerated exposures following oral dosing in healthy volunteers. J Clin Pharmacol. 2017;57:194–210.
22. Kurniawan DW, Jajoriya AK, Dhawan G, Mishra D, Argemi J, Bataller R, et al. Therapeutic inhibition of spleen tyrosine kinase in inflammatory macrophages using PLGA nanoparticles for the treatment of non-alcoholic steatohepatitis. J Control Release. 2018;288:227–38.
23. Daley D, Mani VR, Mohan N, Akkad N, Pandian G, Savadkar S, et al. NLRP3 signaling drives macrophage-induced adaptive immune suppression in pancreatic carcinoma. J Exp Med. 2017;214:1711–24.
24. Ochi A, Nguyen AH, Bedrosian AS, Mushlin HM, Zarbakhsh S, Barilla R, et al. MyD88 inhibition amplifies dendritic cell capacity to promote pancreatic carcinogenesis via Th2 cells. J Exp Med. 2012;209:1671–87.
25. Naugler WE, Sakurai T, Kim S, Maeda S, Kim K, Elsharkawy AM, et al. Gender disparity in liver cancer due to sex differences in MyD88-dependent IL-6 production. Science. 2007;317:121–4.
26. Thapa M, Chinnadurai R, Velazquez VM, Tedesco D, Elrod E, Han JH, et al. Liver fibrosis occurs through dysregulation of MyD88-dependent innate B-cell activity. Hepatology. 2015;61:2067–79.
27. O'Neill LA. A metabolic roadblock in inflammatory macrophages. Cell Rep. 2016;17:625–6.
28. Pradere JP, Troeger JS, Dapito DH, Mencin AA, Schwabe RF. Toll-like receptor 4 and hepatic fibrogenesis. Semin Liver Dis. 2010;30:232–44.
29. Guo J, Friedman SL. Toll-like receptor 4 signaling in liver injury and hepatic fibrogenesis. Fibrogenes Tissue Repair. 2010;3:21.
30. Dapito DH, Mencin A, Gwak GY, Pradere JP, Jang MK, Mederacke I, et al. Promotion of hepatocellular carcinoma by the intestinal microbiota and TLR4. Cancer Cell. 2012;21:504–16.
31. Miller YI, Choi SH, Wiesner P, Bae YS. The SYK side of TLR4: signalling mechanisms in response to LPS and minimally oxidized LDL. Br J Pharmacol. 2012;167:990–9.
32. de Rosamel L, Blanc JF. Emerging tyrosine kinase inhibitors for the treatment of hepatocellular carcinoma. Expert Opin Emerg Drugs. 2017;22:175–90.
33. Llovet JM, Ricci S, Mazzaferro V, Hilgard P, Gane E, Blanc JF, et al. Sorafenib in advanced hepatocellular carcinoma. N Engl J Med. 2008;359:378–90.
34. Inarrairaegui M, Melero I, Sangro B. Immunotherapy of hepatocellular carcinoma: facts and hopes. Clin Cancer Res. 2018;24:1518–24.
35. Wang W, Xu MJ, Cai Y, Zhou Z, Cao H, Mukhopadhyay P, et al. Inflammation is independent of steatosis in a murine model of steatohepatitis. Hepatology. 2017;66:108–23.
36. Zhou Z, Xu MJ, Cai Y, Wang W, Jiang JX, Varga ZV. et al. Neutrophil-hepatic stellate cell interactions promote fibrosis in experimental steatohepatitis. Cell Mol Gastroenterol Hepatol. 2018;5:399–413.
37. Zambirinis CP, Levie E, Nguy S, Avanzi A, Barilla R, Xu Y, et al. TLR9 ligation in pancreatic stellate cells promotes tumorigenesis. J Exp Med. 2015;212:2077–94.
38. Dobin A, Davis CA, Schlesinger F, Drenkow J, Zaleski C, Jha S, et al. STAR: ultrafast universal RNA-seq aligner. Bioinformatics. 2013;29:15–21.
39. Liao Y, Smyth GK, Shi W. Feature Counts: an efficient general purpose program for assigning sequence reads to genomic features. Bioinformatics. 2014;30:923–30.
40. Love MI, Huber W, Anders S. Moderated estimation of fold change and dispersion for RNA-seq data with DESeq2. Genome Biol. 2014;15:550.
41. Shannon P, Markiel A, Ozier O, Baliga NS, Wang JT, Ramage D, et al. Cytoscape: a software environment for integrated models of biomolecular interaction networks. Genome Res. 2003;13:2498–504.